Amino Acids
DOI 10.1007/s00726-012-1369-9

ORIGINAL ARTICLE

Evaluation of a technetium-99m labeled bombesin homodimer for GRPR imaging in prostate cancer

Zilin Yu · Giuseppe Carlucci · Hildo J. K. Ananias · Rudi A. J. O. Dierckx · Shuang Liu · Wijnand Helfrich · Fan Wang · Igle J. de Jong · Philip H. Elsinga

Received: 24 April 2012 / Accepted: 12 July 2012

Abstract Multimerization of peptides can improve the binding characteristics of the tracer by increasing local ligand concentration and decreasing dissociation kinetics. In this study, a new bombesin homodimer was developed based on an ε-aminocaproic acid-bombesin(7–14) (Aca-bombesin(7–14)) fragment, which has been studied for targeting the gastrin-releasing peptide receptor (GRPR) in prostate cancer. The bombesin homodimer was conjugated to 6-hydrazinopyridine-3-carboxylic acid (HYNIC) and labeled with ^{99m}Tc for SPECT imaging. The in vitro binding affinity to GRPR, cell uptake, internalization and efflux kinetics of the radiolabeled bombesin dimer were investigated in the GRPR-expressing human prostate cancer cell line PC-3. Biodistribution and the GRPR-targeting potential were evaluated in PC-3 tumor-bearing athymic nude mice. When compared with the bombesin monomer, the binding affinity of the bombesin dimer is about ten times lower. However, the ^{99m}Tc labeled bombesin dimer showed a three times higher cellular uptake at 4 h after incubation, but similar internalization and efflux characters in vitro. Tumor uptake and in vivo pharmacokinetics in PC-3 tumor-bearing mice were comparable. The tumor was visible on the dynamic images in the first hour and could be clearly distinguished from non-targeted tissues on the static images after 4 h. The GRPR-targeting ability of the ^{99m}Tc labeled bombesin dimer was proven in vitro and in vivo. This bombesin homodimer provides a good starting point for further studies on enhancing the tumor targeting activity of bombesin multimers.

Keywords GRPR · Bombesin homodimer · Radiolabeled · Imaging · Prostate cancer · PC-3 · ^{99m}Tc · HYNIC · SPECT

Z. Yu (✉) · G. Carlucci · R. A. J. O. Dierckx · P. H. Elsinga
Department of Nuclear Medicine and Molecular Imaging, University Medical Center Groningen, University of Groningen, Hanzeplein 1, 9831 EZ Groningen, The Netherlands
e-mail: zilinyu0183@gmail.com

Z. Yu · G. Carlucci · H. J. K. Ananias · I. J. de Jong
Department of Urology, University Medical Center Groningen, University of Groningen, Groningen, The Netherlands

S. Liu
School of Health Sciences, Purdue University, West Lafayette, IN, USA

W. Helfrich
Department of Surgery, Translational Surgical Oncology, University Medical Center Groningen, University of Groningen, Groningen, The Netherlands

F. Wang
Medical Isotopes Research Center, Peking University, Beijing, China

Introduction

Prostate cancer is one of the most common cancers in men in the USA and Europe (Ferlay et al. 2007; Jemal et al. 2008). In the course of the disease, bone metastases will develop in the majority of cases with advanced prostate cancer. This number will reach 90 % in patients with castrate-resistant prostate cancer treated with chemotherapy (Eisenhauer et al. 2009).

At present, there is an unmet need to measure response to treatment of prostate cancer metastases in the skeleton. With a specific radiotracer and specific target in the tumor, positron emission tomography (PET) and single photon emission computed tomography (SPECT) would be powerful diagnostic tools in detection of prostate cancer.

Published online: 26 July 2012

The gastrin-releasing peptide receptor (GRPR) is a subtype of the bombesin receptor family. Mammalian GRPR is preferentially expressed in non-neuroendocrine tissues of the breast and pancreas and in neuroendocrine cells of the brain, gastrointestinal tract and lung (Aprikian et al. 1993; Price et al. 1984; Spindel et al. 1984; Track and Cutz 1982; Xiao et al. 2001). It has also been shown that GRPR is overexpressed in a large variety of human tumors, including prostate, breast, renal and (non) small cell lung cancer. Due to the enhanced expression of GRPR in prostate cancer, GRPR is considered as a potential target for the diagnosis, staging or treatment of prostate cancer.

Bombesin is a 14-amino acid peptide, which was first isolated from the skin of frogs in the 1970 (Erspamer et al. 1970). Bombesin and its mammalian counterpart share seven identical amino acid residues at the C-terminal, which was identified as the binding domain of the bombesin receptor (McDonald et al. 1979).

Radiolabeled bombesin analogs have proven their GRPR-binding ability in several cancer cell lines and various tumor models (Zhang et al. 2006; Shi et al. 2008; Ait-Mohand et al. 2011; Liu et al. 2009d). Previously, an ε-aminocaproic acid (Aca) modified bombesin analog was labeled with ^{18}F and the compound was evaluated in a prostate cancer animal model (Zhang et al. 2006). Although ^{18}F-FB-Aca-bombesin(7–14) showed its ability to target GRPR in an animal model, due to the lipophilic character of the tracer, detection of the orthotopic prostate cancer was hampered by high abdominal background levels.

Recently, we developed HYNIC conjugated Aca-BN(7–14) and labeled it with ^{99m}Tc for SPECT imaging of prostate cancer in an animal model (Ananias et al. 2011). Compared to ^{18}F-FB-Aca-bombesin(7–14), ^{99m}Tc-HYNIC(Tricine/TPPTS)-Aca-BN(7–14) (^{99m}Tc-HABN) showed reduced abdominal background and improved tumor-to-normal tissue (T/NT) contrast (tumor-to-muscle ratio from lower than 5 increased to 13.9 ± 5.9 at 1 h post-injection) on SPECT images.

While most bombesin-like peptides are monomers, we applied the dimerization technology and synthesized a new dimeric bombesin with two identical Aca-bombesin(7–14) units. Multivalent interactions are frequently found in nature where they increase the affinity of weak ligand–receptor interactions such as in the DNA–DNA duplex formation by multiple weak interactions between individual complementary nucleotides, or the typical Y-shaped antibody composed of two heavy chains and two light chains which are joined by disulfide linkages (Kramer and Karpen 1998; Handl et al. 2004; Mulder et al. 2004; Vance et al. 2008). Multivalent structures have become a strategy for the development of drugs and diagnostic agents. It has been shown by several research groups that multivalent compounds are able to enhance the interaction between the ligand and corresponding receptor (Joosten et al. 2004; Liu et al. 2011; Chang et al. 2011; Dijkgraaf et al. 2007, 2011; Shi et al. 2009). One of the most prominent examples is multivalent arginine-glycine-aspartic acid (RGD) analogs. Several isotopes (^{99m}Tc, ^{111}In, ^{18}F, ^{68}Ga, etc.) and chelators (HYNIC, DOTA, DTPA, etc.) have been applied for the preparation of dimeric and tetrameric RGD tracers (Liu et al. 2011; Chang et al. 2011; Dijkgraaf et al. 2007, 2011; Shi et al. 2009). The binding affinity is significantly increased at higher orders of binding valency, a principle usually referred to as avidity. The aim of this study is to investigate the GRPR-targeting characteristics of the bombesin homodimer as a potential imaging agent for prostate cancer.

Materials and methods

Chemicals

Tricine (*N*-(tri(hydroxymethyl)methyl)glycine) was purchased from Sigma/Aldrich (St. Louis, Missouri, USA). Trisodium triphenylphosphine-3,3′,3″-trisulfonate (TPPTS) was purchased from Alfa Aesar (Karlsruhe, Germany). Both were used without further purification. The peptide Glu[Aca-BN(7–14)]$_2$ was provided by Peptides International (Louisville, KY, USA). Na^{99m}TcO$_4$ was eluted from the ^{99}Mo/^{99m}Tc generator MTcG-4 (IAE Radioisotope Centre POLATOM, Świerk, Poland). ^{125}I-Tyr^4-BN was obtained from Perkin-Elmer Life and Analytical Sciences (Waltham, Massachusetts, USA).

Equipment

Semi-preparative reversed-phase high-performance liquid chromatography (RP-HPLC) was performed on a HITACHI L-2130 HPLC system (Hitachi High Technologies America Inc., Pleasanton, CA, USA) equipped with a Bicron Frisk-Tech area monitor. Isolation and quality control of ^{99m}HYNIC(Tricine/TPPTS)-Glu[Aca-BN(7–14)]$_2$ (^{99m}Tc-HABN$_2$) were performed using a Phenomenex reversed-phase Luna C18 column (10 mm × 250 mm, 5 µm) (Torrance, California, USA). The flow was set at 2.5 mL/min using a gradient system starting from 90 % solvent A (0.01 M phosphate buffer, pH 6.0) and 10 % solvent B (acetonitrile) (5 min) and ramped to 45 % solvent A and 55 % solvent B at 35 min (HPLC method 1).

HPLC method 2 used a LabAlliance semi-preparative HPLC system equipped with a UV–Vis detector ($\lambda = 254$ nm) and Zorbax C18 semi-prep column (9.4 mm × 250 mm, 100 Å pore size). The flow rate was 2.5 mL/min. The mobile phase was isocratic with 60 %

solvent A (0.1 % acetic acid in water) and 40 % solvent B (0.1 % acetic acid in acetonitrile) at 0–5 min, followed by a gradient mobile phase going from 60 % solvent A and 40 % solvent B at 5 min to 20 % solvent A and 80 % solvent B at 30 min.

HPLC method 3 used a LabAlliance semi-preparative HPLC system equipped with a UV–Vis detector ($\lambda = 254$ nm) and Zorbax C18 semi-preparative column (9.4 mm × 250 mm, 100 Å pore size). The flow rate was 2.5 mL/min. The gradient mobile phase goes from 90 % solvent A (0.1 % acetic acid in water) and 10 % solvent B (0.1 % acetic acid in acetonitrile) at 0 min to 75 % solvent A at 5 min, followed by a gradient mobile phase going from 75 % solvent A to 65 % solvent A at 40 min.

Synthesis of HYNIC-Glu[Aca-BN(7–14)]$_2$

Sodium succinimidyl 6-(2-(2-sulfonatobenzaldehyde)hydrazono)nicotinate (HYNIC-NHS) was prepared according to the method in literature (Harris et al. 1999).

HYNIC-NHS (21.8 mg, 50 µmol) and Glu[Aca-BN(7–14)]$_2$ (5.8 mg, 2.6 µmol) were dissolved in 1.5 mL of DMF. The pH was adjusted to 8.5–9.0 with DIPEA. The mixture was stirred for 7 days at room temperature to make sure that the reaction was complete as indicated by the disappearance of the peptide peak. The product was purified by HPLC (method 1). The peak of interest at ~28 min was collected. The collected fractions were combined, and lyophilized to obtain 1.7 mg product, which was re-purified by HPLC (method 2). The fraction at ~32.5 min was collected. Lyophilization of the collected fractions gave the final product 0.8 mg (13 %) with a purity >95 % by HPLC. ESI–MS: $C_{114}H_{161}N_{33}O_{27}S_3$, calculated 2,521.9, observed 2,522 ($[M+H]^+$).

Radiochemistry

100 µL of the HYNIC-Glu[Aca-BN(7–14)]$_2$ solution (1 mg/mL in H_2O), 100 µL of tricine solution (50 mg/mL in 25 mM succinate buffer, pH 5.0), 100 µL of TPPTS solution (50 mg/mL in 25 mM succinate buffer, pH 5.0), 5 µL of $SnCl_2$ solution (3.0 mg/mL in 0.1 N HCl) and 100 µL of $Na^{99m}TcO_4$ (370 MBq) in saline were added to a 1.5 mL Eppendorf cup. The Eppendorf cup containing the reaction mixture was sealed and heated at 95 °C for 20 min. After cooling to room temperature, the mixture was purified by HPLC (method 1). The product was then passed through a Waters Sep-Pak C18 light cartridge. ^{99m}Tc-HABN$_2$ was eluted with ethanol (0.4 mL) and diluted with saline solution for in vitro and in vivo experiments. A sample of the resulting solution was analyzed by the same HPLC system (method 1).

Partition coefficient

The partition coefficient was determined using the method described previously (Ananias et al. 2011). The tracer was dissolved in a mixture of 0.5 mL *n*-octanol and 0.5 mL 25 mM phosphate buffer (pH 7.4) and well mixed for 5 min at room temperature. Then the mixture was centrifuged at 3,000 rpm for 5 min; 100 µL samples were obtained from *n*-octanol and aqueous layers. All samples were counted in a γ-counter (Compugamma CS1282, LKB-Wallac, Turku, Finland). The log D value is reported as an average of three different measurements.

In vitro stability

The tracer was dissolved in 1 mL saline or L-cysteine solution (1 mg/mL), incubated at room temperature and analyzed by HPLC (method 1) at 1, 2, 4, 6, and 24 h post-incubation.

Human serum from healthy donors was incubated at 37 °C with ^{99m}Tc-HABN$_2$ for different time periods (1, 2, 4, 6, 24 h). After incubation, a sample of 250 µL was precipitated with 750 µL acetonitrile/ethanol ($V_{acetonitrile}$/$V_{ethanol}$ = 1:1) and then centrifuged (3 min at 3,000 rpm), the supernatants were passed through a Millex-LG filter (Millipore, Co. Cork, Carrigtwohill, Ireland) and afterward analyzed by HPLC (method 1). Results were plotted as radiochemical purity (RCP) at different time points.

Cell culture

The GRPR-positive human prostate cancer cell line PC-3 (ATCC, Manassas, Virginia, USA) was cultured in RPMI 1640 (Lonza, Verviers, France) supplemented with 10 % fetal calf serum (Thermo Fisher Scientific Inc., Logan, UT, USA) at 37 °C in a humidified 5 % CO_2 atmosphere.

In vitro competitive receptor binding assay

The in vitro GRPR binding affinities of Glu[Aca-BN(7–14)]$_2$ and HYNIC-Glu[Aca-BN(7–14)]$_2$ were assessed via a competitive displacement assay with ^{125}I-Tyr^4-BN(1–14) as the GRPR-specific radioligand. Experiments were performed with PC-3 human prostate cancer cells according to a method previously described (Ananias et al. 2011). The 50 % inhibitory concentration (IC_{50}) values were calculated by fitting the data with nonlinear regression using GraphPad Prism 5.0 (GraphPad Software, San Diego, CA, USA). Experiments were performed with triplicate samples. IC_{50} values are reported as an average of these samples plus the standard deviation (SD).

Cellular uptake studies

One day prior to the assay, PC-3 cells at confluence were placed in six-well plates (0.5 million cells/well). The cells were washed twice with PBS solution before using for the experiments. ^{99m}Tc-HABN or ^{99m}Tc-HABN$_2$ (0.0037 MBq/well) was incubated with cells at 37 °C for 0, 15, 30, 45, 60, 90, 120 or 240 min in triplicate to allow for cellular uptake; 20 μg of unlabeled Glu[Aca-BN(7–14)]$_2$ was co-incubated with ^{99m}Tc-HABN or ^{99m}Tc-HABN$_2$ in blocking groups. To remove unbound radioactivity, the cells were washed twice with ice-cold PBS and the cells were lysed by incubation with 1 M NaOH at 37 °C. The resulting lysate in each well was aspirated to determine the uptake of activity with a γ-counter. Results are expressed as percentage of incubated radioactivity (mean ± SD).

Internalization and efflux studies

For the internalization study, 1 million PC-3 cells were placed in six-well plates before the experiments and kept at 37 °C overnight. The cells were washed with PBS and then incubated with ^{99m}Tc-HABN$_2$ (0.0037 MBq/well) for 2 h at 4 °C. To remove unbound radioactivity, the cells were washed twice with ice-cold PBS and incubated with the pre-warmed culture medium at 37 °C for 0, 5, 15, 30, 45, 60, 90 and 120 min in triplicate to allow for internalization.

To remove cell surface-bound radiotracer, the cells were washed twice for 3 min with acid (50 mM glycine–HCl/100 mM NaCl, pH 2.8). The acid solution was collected and measured with a γ-counter. The results were collected as the surface-bound activity. Subsequently, the cells were lysed by incubation with 1 M NaOH at 37 °C and the resulting lysate in each well was measured to determine the internalized radioactivity with a γ-counter. Results are expressed as the percentage of total radioactivity (internalized activity/(surface-bound activity + internalized activity)), (mean ± SD).

For the efflux study, 1 million PC-3 cells were placed in six-well plates 1 day before the experiments and kept at 37 °C. The cells were washed with PBS and then incubated with ^{99m}Tc-HABN$_2$ (3.7 kBq/well) for 1 h at 37 °C to allow for maximum internalization. To remove unbound radioactivity, the cells were washed twice afterward with ice-cold PBS and then incubated in the pre-warmed culture medium at 37 °C for 0, 15, 30, 45, 60, 90, 120 and 240 min in triplicate to allow for externalization. To remove cell surface-bound radiotracer, the cells were washed twice for 3 min with acid (50 mM glycine–HCl/100 mM NaCl, pH 2.8). Then, the cells were lysed by incubation with 1 N NaOH at 37 °C, and the resulting lysate in each well was aspirated to determine the remaining radioactivity in a γ-counter. Results are expressed as the percentage of maximum intracellular radioactivity (remaining activity at specific time point/activity at time point 0) (mean ± SD).

Animal model

In the PC-3 tumor model, 2×10^6 PC-3 cells (suspended in 0.1 mL sterile saline) were subcutaneously injected into the left front flank of male athymic mice (Harlan, Zeist, The Netherlands). During the injection, animals were anesthetized with a gas composed of ~3.5 % isoflurane in an air/oxygen mixture. The mice were used for biodistribution experiments and microSPECT and CT imaging when the tumor volume reached a mean diameter of 0.8–1.0 cm (typically 3–4 weeks after tumor inoculation).

All animal experiments were performed in accordance with the regulations of Dutch law on animal welfare and the institutional ethics committee for animal procedures approved the protocol.

MicroSPECT imaging and biodistribution

The subcutaneous tumor-bearing mice were separated into four groups (4 animals per group) and used for imaging and biodistribution when the tumor volume reached 250–300 mm^3 (4–5 weeks after inoculation).

MicroSPECT scans were performed on a three-head γ-camera (MILabs, U-SPECT-II, Utrecht, The Netherlands) equipped with a multi-pinhole high-resolution collimator. For the microSPECT scans, ~30 MBq ^{99m}Tc-HABN$_2$ was administered by penis vein injection under isoflurane anesthesia; 60 min of dynamic microSPECT data were acquired immediately after injection. Mice (group 1) that were used for dynamic scanning were killed directly after the scan with an overdose of isoflurane anesthesia. CT scan and biodistribution were performed afterward. Blood, tumor, major organs and tissue samples were collected, weighed and counted with γ-counter. The percentage of injected dose per gram (%ID/g) was determined for each sample. For each mouse, radioactivity of the tissue samples was calibrated against a known aliquot of radiotracer.

For static imaging, mice were killed at four (group 2) and 24 h (group 3) after injection. Afterward, 60 min microSPECT and microCT images were acquired. Biodistribution was performed as described above.

For the receptor-blocking experiment 300 μg of unlabeled Aca-BN(7–14) was pre-injected 30 min before the tracer injection. The animals of the blocking group (group 4) were killed and 60-min static microSPECT and CT images were acquired at 4 h after tracer injection. Biodistribution was performed after the CT scan.

Images were reconstructed by using U-SPECT-Rec v 1.34i3 (MILabs, Utrecht, the Netherlands) with a pixel-

based ordered-subsets expectation maximum (POSEM) algorithm. Final images were 1 mm slices, made with Amide 0.9.1 (open source software).

Statistical analysis

Quantitative data are expressed as mean ± SD. Means were compared using the Student's *t* test. p values <0.05 were considered as significant.

Results

Synthesis, radiolabeling, partition coefficient and in vitro stability

^{99m}Tc-HABN$_2$ (Fig. 1) was prepared at 95 °C with moderate labeling yield (>80 %). After purification, the RCP was higher than 95 %. The specific activity was ~17.4 ± 9.7 GBq/μmol ($n = 7$). ^{99m}Tc-HABN$_2$ was well separated from precursor using HPLC system. The retention time (HPLC method 1) of ^{99m}Tc-HABN$_2$ and HYNIC-Glu[Aca-BN(7–14)]$_2$ was around 28 and 24 min, respectively.

The partition coefficient was determined in a mixture of *n*-octanol and phosphate buffer (pH 7.4). The log D value of ^{99m}Tc-HABN$_2$ was −1.54 ± 0.16. The in vitro stability of ^{99m}Tc-HABN$_2$ was evaluated in saline, human serum and in the presence of excess L-cysteine (1.0 mg/mL, pH 7.4) (Fig. 2). ^{99m}Tc-HABN$_2$ was stable in the presence of excess L-cysteine and human serum for at least 4 h (RCP > 95 %). The RCP of ^{99m}Tc-HABN$_2$ in serum slowly decreased to ~84 % after 24 h.

In vitro competitive receptor binding assay

Using ^{125}I-Tyr^4-BN(1–14) as GRPR-specific radioligand, the binding affinities of Glu[Aca-BN(7–14)]$_2$ and HYNIC-Glu[Aca-BN(7–14)]$_2$ for GRPR were compared via an in vitro competitive binding assay. Results are plotted as sigmoid curves for the displacement of ^{125}I-Tyr^4-BN(1–14) as a function of increasing concentrations of Glu[Aca-BN(7–14)]$_2$ and HYNIC-Glu[Aca-BN(7–14)]$_2$ (Fig. 3). The IC_{50} values were found to be 31.4 ± 0.4 nM and 63.4 ± 11.7 nM for Glu[Aca-BN(7–14)]$_2$ and HYNIC-Glu[Aca-BN(7–14)]$_2$, respectively.

Cellular uptake studies

The in vitro uptake of ^{99m}Tc labeled bombesin monomer and dimer in PC-3 cells are shown in Fig. 4. Compared to ^{99m}Tc-HABN, ^{99m}Tc-HABN$_2$ has slower cellular uptake within 30 min of incubation, but keeps accumulating in PC-3 cells over the 4 h experiment period. The highest cellular uptake for ^{99m}Tc-HABN and ^{99m}Tc-HABN$_2$ is 10.9 ± 0.7 % (1 h post-incubation) and 32.5 ± 1.8 % (4 h post-incubation) of added radioactivity, respectively. Co-incubation with excess unlabeled bombesin significantly reduced the cellular uptake of both tracers (<1 % of added activity was belonging to non-specific uptake).

Internalization and efflux studies

The internalization study depicted in Fig. 5a showed rapid internalization of ^{99m}Tc-HABN$_2$ into PC-3 cells within

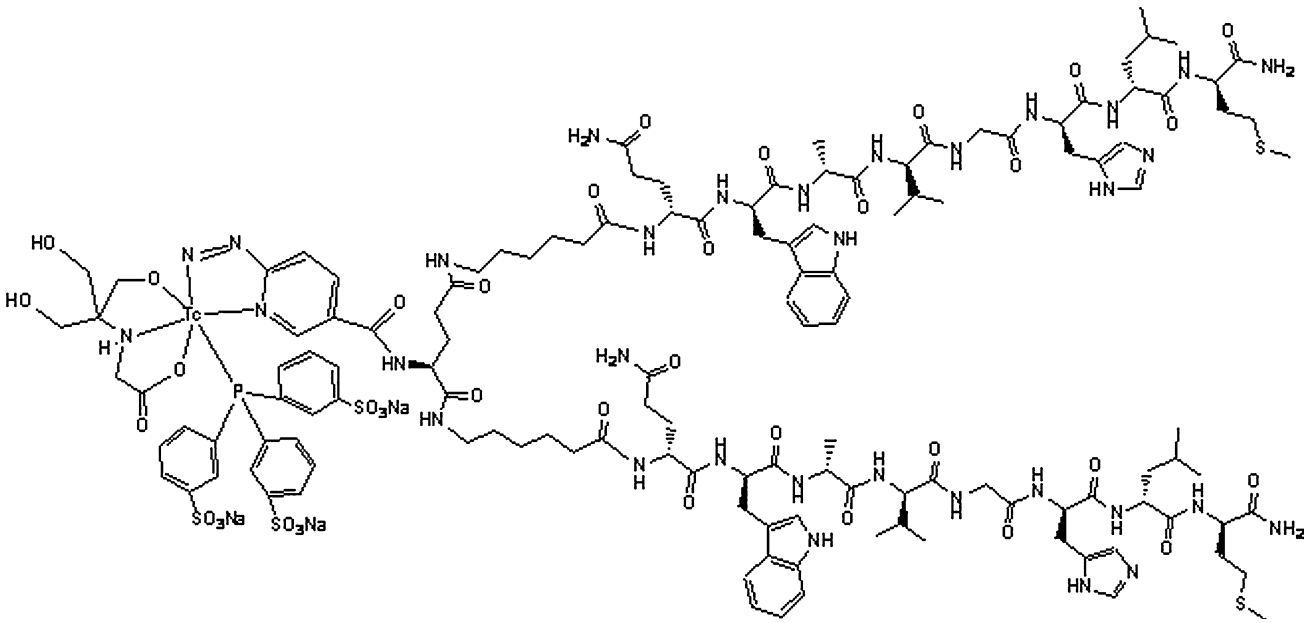

Fig. 1 ^{99m}Tc-HYNIC(Tricine/TPPTS)-Glu[Aca-BN(7–14)]$_2$

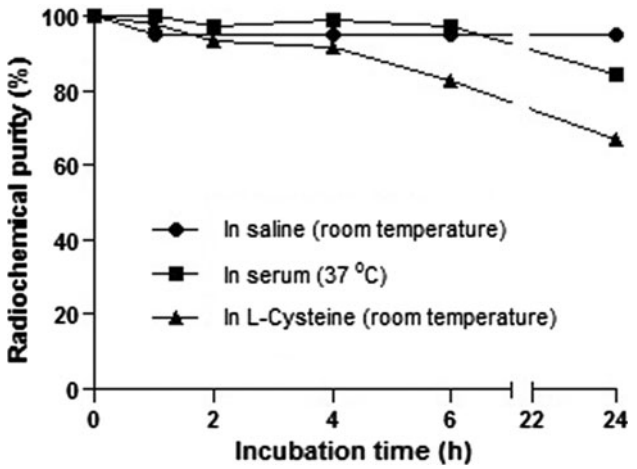

Fig. 2 In vitro stability of ^{99m}Tc-HABN$_2$ in saline (at room temperature), human serum (at 37 °C) and L-cysteine (at room temperature). Results are plotted as the radiochemical purity at different time points

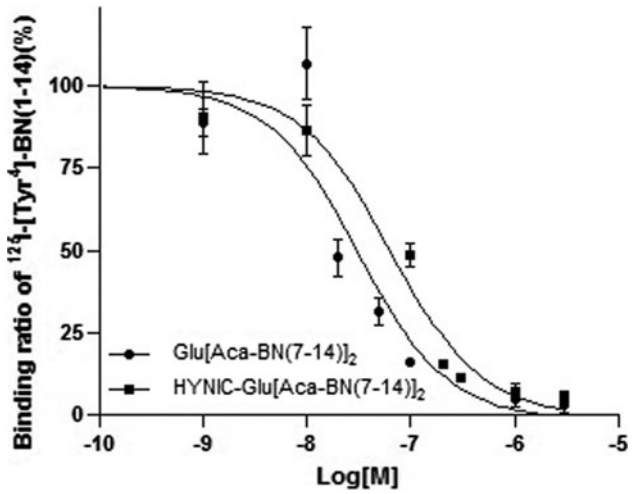

Fig. 3 Inhibition of ^{125}I-[Tyr^4]-BN(1–14) binding to GRPR on PC-3 cells by Glu[Aca-BN(7–14)]$_2$ and HYNIC-Glu[Aca-BN(7–14)]$_2$. Log [M] = log of increasing concentration (mol/L) of Glu[Aca-BN(7–14)]$_2$ and HYNIC-Glu[Aca-BN(7–14)]$_2$

5 min of incubation. The portion of intracellular activity reached a plateau at 15 min post-incubation and 80 % of cell bound activity internalized into the cells.

The results of the efflux study is shown in Fig. 5b. For ^{99m}Tc-HABN$_2$, steady efflux was observed within 2 h of incubation. About 60 % of the intracellular radioactivity was maintained in the cells at the end of the 4 h experiment period. The efflux half-life of ^{99m}Tc-HABN$_2$ was 84 min.

Biodistribution experiments

Biodistribution of ^{99m}Tc-HABN$_2$ was evaluated in athymic nude mice bearing subcutaneous PC-3 tumors after performing the microSPECT and CT scans. The results

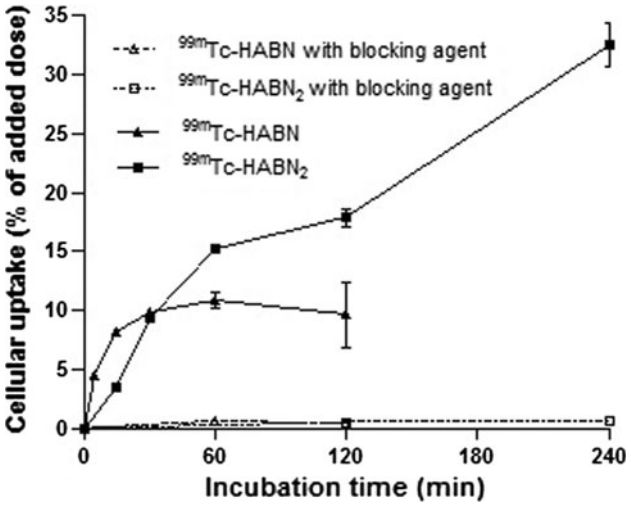

Fig. 4 Cellular uptake assay of ^{99m}Tc-HABN and ^{99m}Tc-HABN$_2$ in PC-3 cells. The cellular uptake results were expressed as percentage added dose ($n = 3$, mean ± SD)

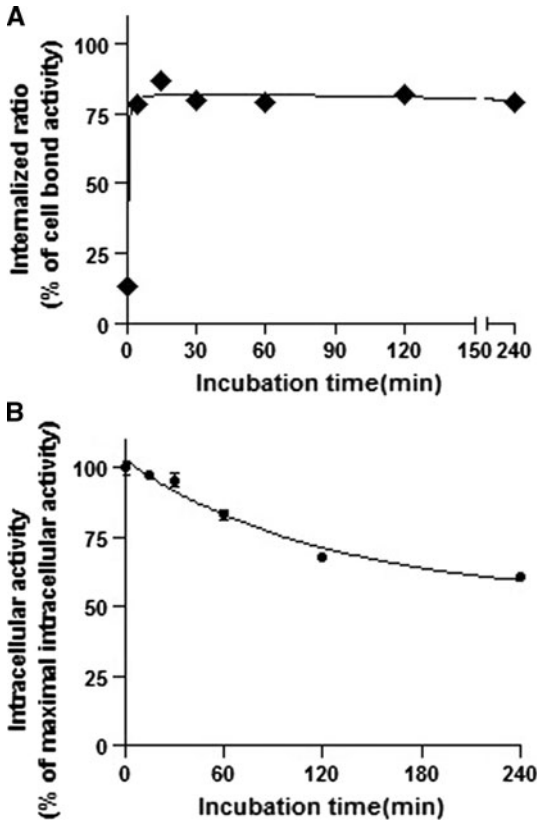

Fig. 5 Internalization (**a**) and efflux (**b**) kinetics of ^{99m}Tc-HABN$_2$ in PC-3 cell line ($n = 3$, mean ± SD)

are shown in Fig. 6. Tumor uptake of ^{99m}Tc-HABN$_2$ was 1.58 ± 0.18 %ID/g at 60 min after injection, with a steady decrease to 0.47 ± 0.13 %ID/g at 24 h after injection. The highest radioactivity uptake (15.1 ± 6.4 %ID/g) in kidney was observed at 4 h post-injection.

The tracer has low blood uptake and was cleared from blood rapidly. The uptake of ^{99m}Tc-HABN$_2$ in non-targeting organs (except kidney and pancreas) such as liver, bone and intestines was lower than 3 %ID/g and washed out rapidly. Due to the slower washout from tumor compared to normal tissue, the T/NT ratio increased during the 24 h experiment period. The tumor-to-muscle ratio increased from 3.7 ± 1.1 at 1 h after injection to 24.1 ± 21.5 at 24 h after injection.

For determining the specificity of ^{99m}Tc-HABN$_2$ binding to GRPR, an excess of unlabeled Aca-BN(7–14) (300 μg/mouse) was injected before the tracer injection. At 4 h post-injection, the radioactivity accumulation was substantially reduced in tumor (from 0.8 ± 0.3 to 0.4 ± 0.1 %ID/g) and pancreas (from 9.6 ± 7.6 to 3.1 ± 0.2 %ID/g).

MicroSPECT imaging

Typical microSPECT images of PC-3 tumor-bearing mice at different time points after tracer injection are shown in Fig. 7. The tumors were clearly visible from static miro-SPECT images acquired at 4 h after injection of ^{99m}Tc-HABN$_2$ (b). Prominent uptake of ^{99m}Tc-HABN$_2$ was also observed in the kidneys and pancreas at all images during the 4 h experiment period (a, b). With excess blocking agent (Aca-BN(7–14), 300 μg/mouse), significant reduction of tumor uptake was observed from the images of the

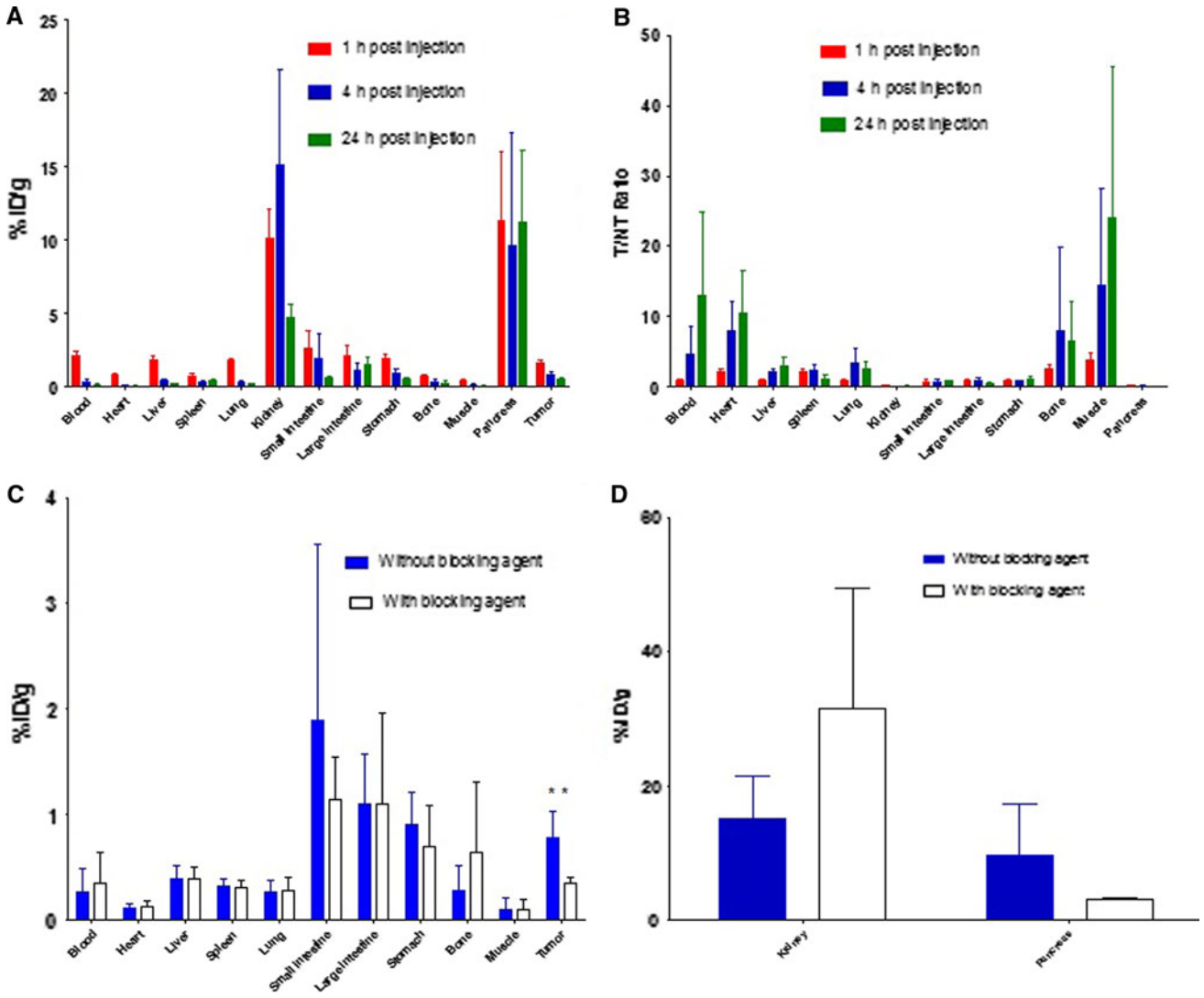

Fig. 6 **a** Biodistribution of ^{99m}Tc-HABN$_2$ at 1, 4, 24 h post-injection in athymic nude mice bearing subcutaneous PC-3 tumor (mean ± SD %ID/g), **b** T/NT ratio of ^{99m}Tc-HABN$_2$ at 1, 4, 24 h post-injection (mean ± SD), **c** biodistribution of ^{99m}Tc-HABN$_2$ at 4 h post-injection with and without blocking agent (mean ± SD %ID/g), **d** uptake of ^{99m}Tc-HABN$_2$ in kidney and pancreas at 4 h post-injection with and without blocking agent (mean ± %ID/g). *Statistically significant difference ($p < 0.05$)

blocking group(c), but kidney and bladder (urine) uptake remained high.

Discussion

Dimerization was applied to evaluate a new dimeric bombesin with two identical Aca-bombesin(7–14) units for its GRPR-targeting characteristics as a potential imaging agent for prostate cancer. A side by side comparison of the in vitro and in vivo behavior of monomer and dimer is listed in Table 1.

In a comparative binding assay, bombesin dimer replaced 50 % binding of ^{125}I-tyr^4-BN(1–14) from the GRP receptors in relatively higher nanomolar concentration (31.4 ± 0.4 nM) than the corresponding monomer (Ananias et al. 2011). HYNIC conjugation showed similar slightly negative effect on binding affinity of HYNIC-Glu[Aca-BN(7–14)]$_2$. The additional Aca-BN(7–14) motif and the linker may not be sufficiently flexible to fit in the binding pocket of the GRP receptor as compared to the monomer. The linker may be too short, thereby causing steric hindrance upon binding of the molecule to the receptor. However, the IC_{50} of HYNIC-Glu[Aca-BN(7–14)]$_2$ is still in an acceptable range. Thus, we decided to label bombesin homodimer with ^{99m}Tc for in vitro and in vivo characterizations.

Although development of PET facilities and radiotracers for PET imaging is blooming nowadays, developing new tracers for SPECT imaging is still important because of the availability of SPECT in most areas all over the world. Due to the favorable radioisotope characters and widespread clinical use, we chose to use the γ-emitting isotope ^{99m}Tc. As we reported in previous study (Ananias et al. 2011), the HYNIC/tricine/TPPTS complex was used to serve as chelator for our new tracer because of its high labeling efficiency (rapid and high yield radiolabeling), high solution stability and relatively easy use (Shi et al. 2008; Ananias et al. 2011; Liu et al. 2008). It was also chosen because of its hydrophilic character leading to the preferred excretion route via the renal–urinary system. Although urinary activity can limit the clinical use in the pelvic and retroperitoneal areas, this limitation will not be relevant for evaluation of metastases in the skeleton.

^{99m}Tc-HABN$_2$ was prepared with high purity. Due to the same ^{99m}Tc labeling core, monomer and dimer shared similar character in labeling, hydrophilicity and solution stability in saline, cysteine and human serum. However, we noticed that several days of incubation was necessary to complete the conjugation of the HYNIC chelator to the bombesin homodimer due to the position of active glutamic acid. The slightly lower rate of ^{99m}Tc-HYNIC(Tricine/TPPTS)-Glu[Aca-BN(7–14)]$_2$ complex construction may be caused for the same reason.

The in vitro cellular uptake, internalization and efflux kinetics were evaluated using the GRPR-expressing human prostate cancer cell line PC-3. Although the binding affinity of bombesin homodimer was ten times lower than monomer, the specific accumulation of ^{99m}Tc-HABN$_2$ showed almost a linear increase during 4 h of experiment period with the highest cellular uptake of 32.5 ± 1.8 % added activity (threefold as high as that of ^{99m}Tc-HABN), whereas that of ^{99m}Tc-HABN reached an uptake plateau in 30 min, which may be due to the higher bombesin "local concentration" of the homodimer in the vicinity of the receptor. In the in vitro competitive receptor binding assay, PC-3 cells were incubated with the bombesin ligands for 1 h to allow for the replacement of the GRPR-bound of ^{125}I-tyr^4-BN(1–14). Cellular uptake of ^{99m}Tc-HABN$_2$ gradually increased over time and became higher than ^{99m}Tc-HABN only after 1 h post-incubation. This finding indicated that ^{99m}Tc-HABN$_2$ may be more suitable for cancer imaging at later time points (for example 4, 24 h p.i.). Therefore, we decided to evaluate the biodistribution and SPECT imaging characters of radiolabeled homodimer in a human prostate cancer xenograft bearing mouse animal model till 24 h post-injection.

For ^{99m}Tc-HABN and ^{99m}Tc-HABN$_2$, tumors were visualized in the first time frame of microSPECT image at 10 min post-injection. It reflected the rapid receptor

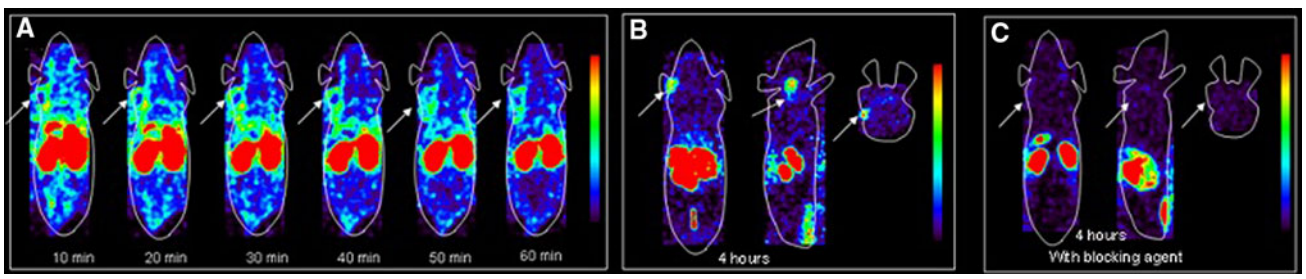

Fig. 7 Dynamic coronal microSPECT images of ^{99m}Tc-HABN$_2$ on PC-3 tumor-bearing athymic mice during first hour after injection without blocking agent (**a**) (10 min/frame). Static coronal, sagittal and axial images of ^{99m}Tc-HABN$_2$ on PC-3 tumor-bearing mice without (**b**) and with blocking agent (**c**) at 4 h after injection. *Arrows* pointed at the tumor

Table 1 Comparison of the in vitro and in vivo behavior of bombesin monomer (Ananias et al. 2011) and dimer

	^{99m}Tc-HABN	^{99m}Tc-HABN$_2$
IC_{50} (nM)[a]	12.81 ± 1.34	63.40 ± 11.70
In vitro stability (in human serum)	Stable at 6 h	Stable at 6 h
Log D value	−1.60 ± 0.06	−1.54 ± 0.16
Highest cellular uptake (% of incubation dose)	10.9 ± 0.7[b]	32.5 ± 1.8[c]
Half-life of efflux (min)	37	84
Tumor uptake (%ID/g)	1.51 ± 0.38	1.58 ± 0.18
Kidney uptake (%ID/g)	6.39 ± 0.83	10.07 ± 1.76
Pancreas uptake (%ID/g)	8.92 ± 1.74	11.26 ± 4.11
Tumor-to-muscle ratio	13.92	3.70

Uptake values (in %ID/g) and T/NT ratios are determined in several organs and PC-3 tumor at 1 h p.i. unless stated otherwise

[a] IC_{50} determined with HYNIC conjugations (HYNIC-Aca-BN(7–14) or HYNIC-Glu[Aca-BN(7–14)]$_2$)

[b] Cellular uptake value determined at 1 h post-incubation

[c] Cellular uptake value determined at 4 h post-incubation

binding and internalization via GRPR. The slightly higher tumor uptake of ^{99m}Tc-HABN$_2$ (0.78 ± 0.26 %ID/g) compared to ^{99m}Tc-HABN (0.67 ± 0.26 %ID/g) at 4 h post-injection could be attributed to the combination of higher cellular uptake, slower efflux and molecular size effect. Instead of steady decreases over time, the uptake of ^{99m}Tc-HABN$_2$ remains constantly high (11.2 ± 4.9 %ID/g at 24 h post-injection) in the pancreas which may be because of the same reasons.

Not only in the GRPR-expressing tissues, but also in the non-GRPR tissues the ^{99m}Tc-HABN$_2$ showed a longer retention compared to ^{99m}Tc-HABN. The apparent increase in molecular size resulted in an increased circulation time and slower clearance of the bombesin dimer. The accumulation in blood for ^{99m}Tc-HABN$_2$ was four times higher as that for ^{99m}Tc-HABN at 1 h post-injection. Although T/NT ratios were constantly increasing due to the slower excretion of ^{99m}Tc-HABN$_2$ in tumor than in non-target tissues (Fig. 6), it was well feasible to visualize the tumor with the SPECT images till 4 h post-injection. The contrast of tumor in SPECT images is expected to be better at 24 h post-injection, but due to the short half-life of ^{99m}Tc, it was not possible to perform the SPECT scan at 24 h post-injection.

Because of the doubled positive charge from 2 Aca-BN(7–14) motifs, the radioactivity accumulation of ^{99m}Tc-HABN$_2$ in kidney remains at high level within 24 h, with the highest accumulation of 15.1 ± 6.4 %ID/g at 4 h post-injection and decrease to 4.7 ± 0.9 %ID/g at 24 h. The high radioactivity accumulation in kidney and urine observed from SPECT imaging and/or biodistribution results indicates that the ^{99m}Tc-HABN$_2$ was excreted through the renal–urine pathway which is consistent with other ^{99m}Tc-HYNIC-peptides.

The agonist property of ^{99m}Tc-HABN$_2$ was confirmed by its rapid internalization. Although it is still unclear which of the agonists and antagonists are more suitable for the imaging of GRPR-expressing cancer, a few radiolabeled bombesin antagonists, such as demobesin-1 (Schroeder et al. 2010), have already showed their superiority to agonists in tumor accumulation, retention of radioactivity and in vivo pharmacokinetics. Compared to those antagonists, ^{99m}Tc-HABN$_2$ exhibited comparable tumor accumulation, but less favorable pharmacokinetics. Further studies which focus on improving the binding affinity and pharmacokinetics of bombesin homodimer are underway.

Recently, a series of radiolabeled arginine-glycine-aspartic acid–bombesin (RGD–BBN) heterodimers for the GRPR targeting were reported (Liu et al. 2009a, b, c, d; Li et al. 2008). Those heterodimers aim at targeting two types of receptors simultaneously, to enhance tumor contrast when either or both receptor types are expressed. In the RGD–BBN heterodimer molecule containing one bombesin motif and one RGD motif, the RGD motif is responsible for targeting integrin $\alpha_v\beta_3$-receptors which are upregulated on activated tumor endothelial cells and also highly expressed on some tumor cells such as glioblastoma, breast and prostate tumors, malignant melanomas and ovarian carcinomas (Hynes 2002). Compared to the bombesin monomer or RGD monomer, the heterodimer shows a synergistic effect for in vivo PC-3 tumor targeting in an animal model (Li et al. 2008). However, using heterodimers, the target specificity of the SPECT or PET image is lost, but general detection of tumor lesions may be improved. The RGD–BBN heterodimer labeled with radiometals (^{68}Ga and ^{64}Cu) showed higher background than ^{18}F-labeled tracer, but slower washout and higher tumor uptake in nude mice bearing breast tumors (Liu et al. 2009d). It is worth exploring the potency of different radioisotopes and chelators on the binding properties and pharmacokinetics of bombesin homodimers.

Within ^{99m}Tc-HABN$_2$, two identical bombesin ligands were conjugated with glutamic acid. Based on the results described in this paper, it is not possible for the two bombesin moieties to bind to GRPR simultaneously. It would be interesting to investigate the effects of linkers with differences in length, lipophilicity and flexibility, on the in vitro and in vivo behavior of the tracer.

Conclusions

We successfully developed a ^{99m}Tc-labeled homodimeric bombesin tracer which showed binding with acceptable

affinity and specificity to the GRP receptor-positive PC-3 prostate cancer cells in vitro and in vivo. Moreover, we have shown its ability for tumor imaging. Further studies on modification of homodimeric bombesin are required. The current dimer is a useful lead compound for this purpose.

Acknowledgments This work was made possible by a financial contribution from CTMM, project PCMM, project number 03O-203. We thank Chao Wu for technical assistance on microSPECT images reconstruction and D.F. Samplonius for technical assistance on cell culturing, and J. W. A. Sijbesma for assisting with animal experiments. All animal experiments were approved by the local animal welfare committee in accordance with the Dutch legislation and carried out in accordance with their guidelines.

References

Ait-Mohand S, Fournier P, Dumulon-Perreault V, Kiefer GE, Jurek P, Ferreira CL, Benard F, Guerin B (2011) Evaluation of 64Cu-labeled bifunctional chelate–bombesin conjugates. Bioconjug Chem 22(8):1729–1735. doi:10.1021/bc2002665

Ananias HJ, Yu Z, Dierckx RA, van der Wiele C, Helfrich W, Wang F, Yan Y, Chen X, de Jong IJ, Elsinga PH (2011) (99m)technetium-HYNIC(tricine/TPPTS)-Aca-bombesin(7–14) as a targeted imaging agent with microSPECT in a PC-3 prostate cancer xenograft model. Mol Pharm 8(4):1165–1173. doi:10.1021/mp200014h

Aprikian AG, Cordon-Cardo C, Fair WR, Reuter VE (1993) Characterization of neuroendocrine differentiation in human benign prostate and prostatic adenocarcinoma. Cancer 71(12):3952–3965

Chang E, Liu S, Gowrishankar G, Yaghoubi S, Wedgeworth JP, Chin F, Berndorff D, Gekeler V, Gambhir SS, Cheng Z (2011) Reproducibility study of [(18)F]FPP(RGD)2 uptake in murine models of human tumor xenografts. Eur J Nucl Med Mol Imaging 38(4):722–730. doi:10.1007/s00259-010-1672-1

Dijkgraaf I, Kruijtzer JA, Liu S, Soede AC, Oyen WJ, Corstens FH, Liskamp RM, Boerman OC (2007) Improved targeting of the alpha(v)beta (3) integrin by multimerisation of RGD peptides. Eur J Nucl Med Mol Imaging 34(2):267–273. doi:10.1007/s00259-006-0180-9

Dijkgraaf I, Yim CB, Franssen GM, Schuit RC, Luurtsema G, Liu S, Oyen WJ, Boerman OC (2011) PET imaging of alphavbeta integrin expression in tumours with Ga-labelled mono-, di- and tetrameric RGD peptides. Eur J Nucl Med Mol Imaging 38(1):128–137. doi:10.1007/s00259-010-1615-x

Eisenhauer EA, Therasse P, Bogaerts J, Schwartz LH, Sargent D, Ford R, Dancey J, Arbuck S, Gwyther S, Mooney M, Rubinstein L, Shankar L, Dodd L, Kaplan R, Lacombe D, Verweij J (2009) New response evaluation criteria in solid tumours: revised RECIST guideline (version 1.1). Eur J Cancer 45(2):228–247. doi:10.1016/j.ejca.2008.10.026

Erspamer V, Erpamer GF, Inselvini M (1970) Some pharmacological actions of alytesin and bombesin. J Pharm Pharmacol 22(11):875–876

Ferlay J, Autier P, Boniol M, Heanue M, Colombet M, Boyle P (2007) Estimates of the cancer incidence and mortality in Europe in 2006. Ann Oncol 18(3):581–592. doi:10.1093/annonc/mdl498

Handl HL, Vagner J, Yamamura HI, Hruby VJ, Gillies RJ (2004) Lanthanide-based time-resolved fluorescence of in cyto ligand–receptor interactions. Anal Biochem 330(2):242–250. doi:10.1016/j.ab.2004.04.012

Harris TD, Sworin M, Williams N, Rajopadhye M, Damphousse PR, Glowacka D, Poirier MJ, Yu K (1999) Synthesis of stable hydrazones of a hydrazinonicotinyl-modified peptide for the preparation of 99m Tc-labeled radiopharmaceuticals. Bioconjug Chem 10(5):808–814 pii:bc9900237

Hynes RO (2002) Integrins: bidirectional, allosteric signaling machines. Cell 110(6):673–687 pii: S0092867402009716

Jemal A, Siegel R, Ward E, Hao Y, Xu J, Murray T, Thun MJ (2008) Cancer statistics. CA Cancer J Clin 58(2):71–96. doi:10.3322/CA.2007.0010

Joosten JA, Loimaranta V, Appeldoorn CC, Haataja S, El Maate FA, Liskamp RM, Finne J, Pieters RJ (2004) Inhibition of *Streptococcus suis* adhesion by dendritic galabiose compounds at low nanomolar concentration. J Med Chem 47(26):6499–6508. doi:10.1021/jm049476+

Kramer RH, Karpen JW (1998) Spanning binding sites on allosteric proteins with polymer-linked ligand dimers. Nature 395(6703):710–713. doi:10.1038/27227

Li ZB, Wu Z, Chen K, Ryu EK, Chen X (2008) 18F-labeled BBN-RGD heterodimer for prostate cancer imaging. J Nucl Med 49(3):453–461. doi:10.2967/jnumed.107.048009

Liu S, Kim YS, Hsieh WY, Gupta Sreerama S (2008) Coligand effects on the solution stability, biodistribution and metabolism of the (99m)Tc-labeled cyclic RGDfK tetramer. Nucl Med Biol 35(1):111–121. doi:10.1016/j.nucmedbio.2007.08.006

Liu Z, Li ZB, Cao Q, Liu S, Wang F, Chen X (2009a) Small-animal PET of tumors with (64)Cu-labeled RGD–bombesin heterodimer. J Nucl Med 50(7):1168–1177. doi:10.2967/jnumed.108.061739

Liu Z, Niu G, Wang F, Chen X (2009b) (68)Ga-labeled NOTA-RGD–BBN peptide for dual integrin and GRPR-targeted tumor imaging. Eur J Nucl Med Mol Imaging 36(9):1483–1494. doi:10.1007/s00259-009-1123-z

Liu Z, Yan Y, Chin FT, Wang F, Chen X (2009c) Dual integrin and gastrin-releasing peptide receptor targeted tumor imaging using 18F-labeled PEGylated RGD–bombesin heterodimer 18F-FB-PEG3-Glu-RGD–BBN. J Med Chem 52(2):425–432. doi:10.1021/jm801285t

Liu Z, Yan Y, Liu S, Wang F, Chen X (2009d) (18)F, (64)Cu, and (68)Ga labeled RGD–bombesin heterodimeric peptides for PET imaging of breast cancer. Bioconjug Chem 20(5):1016–1025. doi:10.1021/bc9000245

Liu Z, Shi J, Jia B, Yu Z, Liu Y, Zhao H, Li F, Tian J, Chen X, Liu S, Wang F (2011) Two Y-labeled multimeric RGD peptides RGD4 and 3PRGD2 for integrin targeted radionuclide therapy. Mol Pharm 8(2):591–599. doi:10.1021/mp100403y

McDonald TJ, Jornvall H, Nilsson G, Vagne M, Ghatei M, Bloom SR, Mutt V (1979) Characterization of a gastrin releasing peptide from porcine non-antral gastric tissue. Biochem Biophys Res Commun 90(1):227–233 pii:0006-291X(79)91614-0

Mulder A, Huskens J, Reinhoudt DN (2004) Multivalency in supramolecular chemistry and nanofabrication. Org Biomol Chem 2(23):3409–3424. doi:10.1039/b413971b

Price J, Penman E, Wass JA, Rees LH (1984) Bombesin-like immunoreactivity in human gastrointestinal tract. Regul Pept 9(1–2):1–10

Schroeder RP, Muller C, Reneman S, Melis ML, Breeman WA, de Blois E, Bangma CH, Krenning EP, van Weerden WM, de Jong M (2010) A standardised study to compare prostate cancer targeting efficacy of five radiolabelled bombesin analogues. Eur J Nucl Med Mol Imaging 37(7):1386–1396. doi:10.1007/s00259-010-1388-2

Shi J, Jia B, Liu Z, Yang Z, Yu Z, Chen K, Chen X, Liu S, Wang F (2008) 99mTc-labeled bombesin(7–14)NH2 with favorable properties for SPECT imaging of colon cancer. Bioconjug Chem 19(6):1170–1178. doi:10.1021/bc700471z

Shi J, Kim YS, Zhai S, Liu Z, Chen X, Liu S (2009) Improving tumor uptake and pharmacokinetics of (64)Cu-labeled cyclic RGD peptide dimers with Gly(3) and PEG(4) linkers. Bioconjug Chem 20(4):750–759. doi:10.1021/bc800455p

Spindel ER, Chin WW, Price J, Rees LH, Besser GM, Habener JF (1984) Cloning and characterization of cDNAs encoding human gastrin-releasing peptide. Proc Natl Acad Sci USA 81(18): 5699–5703

Track NS, Cutz E (1982) Bombesin-like immunoreactivity in developing human lung. Life Sci 30(18):1553–1556

Vance D, Shah M, Joshi A, Kane RS (2008) Polyvalency: a promising strategy for drug design. Biotechnol Bioeng 101(3):429–434. doi:10.1002/bit.22056

Xiao D, Wang J, Hampton LL, Weber HC (2001) The human gastrin-releasing peptide receptor gene structure, its tissue expression and promoter. Gene 264(1):95–103. doi:10.1016/S0378-1119(00)00596-5

Zhang X, Cai W, Cao F, Schreibmann E, Wu Y, Wu JC, Xing L, Chen X (2006) 18F-labeled bombesin analogs for targeting GRP receptor-expressing prostate cancer. J Nucl Med 47(3):492–501